Journal of Biomechanics 77 (2018) 206–210

Contents lists available at ScienceDirect

Journal of Biomechanics

journal homepage: www.elsevier.com/locate/jbiomech
www.JBiomech.com

Short communication

Development of a dynamic index finger and thumb model to study impairment

Alexander J. Barry [a,*], Wendy M. Murray [a,b,c,d,e], Derek G. Kamper [c,f,g]

[a] Shirley Ryan AbilityLab, Chicago, IL, United States
[b] Department of Biomedical Engineering, Northwestern University, Evanston, IL, United States
[c] Department of Physical Medicine & Rehabilitation, Northwestern University Feinberg School of Medicine, Chicago, IL, United States
[d] Department of Physical Therapy and Human Movement Sciences, Northwestern University Feinberg School of Medicine, Chicago, IL, United States
[e] Edward Hines, Jr. VA Hospital, Hines, IL, United States
[f] UNC/NC State Joint Department of Biomedical Engineering, North Carolina State University, Raleigh, NC, United States
[g] Closed-Loop Engineering for Advanced Rehabilitation Research Core, North Carolina State University, Raleigh, NC, United States

ARTICLE INFO

Article history:
Accepted 19 June 2018

Keywords:
Musculoskeletal modelling
Hand
Stroke

ABSTRACT

Modeling of the human hand provides insight for explaining deficits and planning treatment following injury. Creation of a dynamic model, however, is complicated by the actions of multi-articular tendons and their complex interactions with other soft tissues in the hand. This study explores the creation of a musculoskeletal model, including the thumb and index finger, to explore the effects of muscle activation deficits. The OpenSim model utilizes physiological axes of rotation at all joints, passive joint torques, and appropriate moment arms. The model was validated through comparison with kinematic and kinetic experimental data. Simulated fingertip forces resulting from modeled musculotendon loading largely fell within one standard deviation of experimental ranges for most index finger and thumb muscles, although agreement in the sagittal plane was generally better than for the coronal plane. Input of experimentally obtained electromyography data produced the expected simulated finger and thumb motion. Use of the model to predict the effects of activation deficits on pinch force production revealed that the intrinsic muscles, especially first dorsal interosseous (FDI) and adductor pollicis (ADP), had a substantial impact on the resulting fingertip force. Reducing FDI activation, such as might occur following stroke, altered fingertip force direction by up to 83° for production of a dorsal fingertip force; reducing ADP activation reduced force production in the thumb by up to 62%. This validated model can provide a means for evaluating clinical interventions.

1. Introduction

Almost 20 million Americans report some measure, often severe, of hand impairment (Ficke et al., 1992). The ability to simulate potential interventions and their impact on hand kinematics and dynamics would be highly beneficial for rehabilitation. Previously, researchers have developed a number of models to describe properties of the digits, including tendon pathways and moment arms (An et al., 1983, Landsmeer, 1961), isometric force generation at the fingertip (Valero-Cuevas et al., 1998) and thumb-tip (Valero-Cuevas et al., 2003, Wohlman, 2015). Dynamic models of the index finger (Esteki and Mansour, 1997, Lee and Zhang, 2007, Sancho-Bru et al., 2001, Sancho-Bru et al., 2003, Vignais et al., 2013) and thumb have enlightened description of the translation of muscle activation to movement (Ajiboye and Weir 2009, Blana et al., 2017, Klein Breteler et al., 2007).

While these previous models have examined many key aspects of hand motor control, a fully comprehensive model, including crucial representations of all digit degrees-of-freedom (DOF), physiological axes of rotation, and passive mechanics, is lacking. Published models have not fully captured the non-orthogonal, non-intersecting axes of the thumb and fingers seen experimentally (Hollister et al., 1992, Hollister and Giurintano, 1993, Hollister et al., 1995). The alignments of these rotational axes allow for unique, functional movements, such as opposition between the thumb and fingers.

Our goal was to create such a model of the thumb and index finger, the most functionally important and independent digits

* Corresponding author at: 355 E Erie St., 22nd Floor Shirley Ryan AbilityLab, Chicago, IL, 60611, United States.
E-mail address: abarry@sralab.org (A.J. Barry).

https://doi.org/10.1016/j.jbiomech.2018.06.017
0021-9290/

(Almecija et al., 2010, Hager-Ross and Schieber, 2000, Young, 2003). Model performance was validated through comparison with experimental data. The validated model was then used to estimate the relative impact of changes in muscle activation on fingertip/thumb-tip force generation, as might occur following stroke (Hoffmann et al., 2016, Li et al., 2014, Triandafilou et al., 2011). These simulations show the sensitivity of each muscle on force production, thereby providing a better guide for future rehabilitation efforts.

2. Methods

2.1. Model design

The model was developed using OpenSim 3.3 (Stanford, CA), an open-source musculoskeletal platform. The bone geometries used in this model were made available in the OpenSim distribution site by a previous study (Holzbaur et al., 2005).

The physiological, non-orthogonal joint axes of rotation were included in the model by specifying axis orientations for each joint. For joints with more than one DOF, a massless body was inserted into the kinematic chain to permit the second rotation. Thus, the index finger in this model had four DOF and the thumb had five DOF. The anatomical axes of rotation employed in the model were derived from literature descriptions of the index finger and thumb (Hollister et al., 1992, Hollister and Giurintano, 1993, Hollister et al., 1995). Carpal rotations of the index finger, shown to be small (Buffi et al., 2013), were not modeled.

Passive stiffness was included as position-dependent torques for all flexion/extension DOF of the index finger, as well as thumb carpometacarpophalangeal (CMC) abduction (Domalain et al., 2010, Kamper et al., 2002, Knutson et al., 2000). As no such data set could be found for the passive properties of thumb metacarpophalangeal (MCP) and interphalangeal (IP) joint stiffness, their values were set equal to those of index finger MCP and proximal interphalangeal (PIP) joints.

Musculotendons were simulated by geometrically routing representations with via points (Fig. 1a), muscles included are listed in Table 1. For first dorsal interosseous (FDI) and adductor pollicis (ADP) we employed two heads, lateral and medial for FDI, and oblique and transverse for ADP. We used wrapping surfaces to ensure proper pathways around joints (Fig. 1b). These ellipsoids and cylinders were created to match moment arms described in literature (An et al., 1983, Qiu et al., 2017, Smutz et al., 1998).

Muscle force was computed using a Hill-type, "damped equilibrium", muscle model (Delp et al., 2007, Millard et al., 2013), available in the OpenSim environment. Most parameter values for the model were obtained from literature, including: physiological cross sectional area and specific muscle tension (Jacobson et al., 1992, Mogk et al., 2011, Triandafilou and Kamper, 2012, Wohlman and Murray, 2013), optimal fiber length (Holzbaur et al., 2005, Jacobson et al., 1992, Stamenkovic et al., 2014), and pennation angle (Jacobson et al., 1992, Lieber et al., 1992). Slack length was calculated from musculotendon length and muscle length (Eq. (1)):

Table 1
Muscles used to represent the index finger and thumb in this model.

Index Finger Muscles	Thumb Muscles
Flexor digitorum superficialis (FDS)	Flexor pollicis longus (FPL)
Flexor digitorum profundus (FDP)	Flexor pollicis brevis (FPB)
Extensor digitorum communis (EDC)	Extensor pollicis longus (EPL)
Extensor indicis (EI)	Extensor pollicis brevis (EPB)
Lumbrical (LUM)	Abductor pollicis longus (APL)
First palmar interosseous (FPI)	Abductor pollicis brevis (APB)
First dorsal interosseous (FDI)	Opponens pollicis (OPP)
	Adductor pollicis (ADP)

$$l_s^T = \frac{l_{MT}\left(\overrightarrow{\theta}_i = \overrightarrow{0}^\circ\right) - l_M^\circ \cos(\alpha)}{1.033} \quad (1)$$

where $l_{MT}(\theta_i = 0^\circ)$: musculotendon length when all joints crossed by the musculotendon are equal to 0° and the muscle is inactive; l_M^o: optimal fiber length; and α: pennation angle. Strain was set to 3.3%, the end of the toe region on the length-tension curve (Wohlman, 2015). Joint torque produced by each muscle is computed from these parameters, in conjunction with muscle activation level, standard muscle force-length curve (Millard et al., 2013), standard force-velocity curve (Thelen et al., 2003), and moment arm.

2.2. Model validations

Isometric resultant forces produced at the fingertip/thumb-tip in the model were compared in magnitude and direction with published experimental results measured from cadaver specimens. The index finger was compared to ±1 SD of experimental data (Qiu et al., 2017), and the thumb was compared to the interquartile range (IQR) or 50% of reported results (Towles et al., 2008). For the simulations, each muscle was loaded with forces equivalent to those used experimentally; joint posture for the model, a key determinant of force production, was set to match the cadaveric experiments.

As measuring isometric force values is not a native function of OpenSim, a massless sphere was added at the digit tip, constrained by frictionless walls in all three dimensions (Fig. 1c). The contact between the sphere and walls ensured that force production would be applied in the appropriate direction, a method described previously (Valero-Cuevas et al., 1998).

Dynamic simulations were run using published EMG data to predict index finger and thumb motion during grasping and pinch, respectively (Qiu and Kamper, 2014, Valero-Cuevas et al., 2003). As quantitative kinematic data were not reported in this literature, we visually assessed these motions.

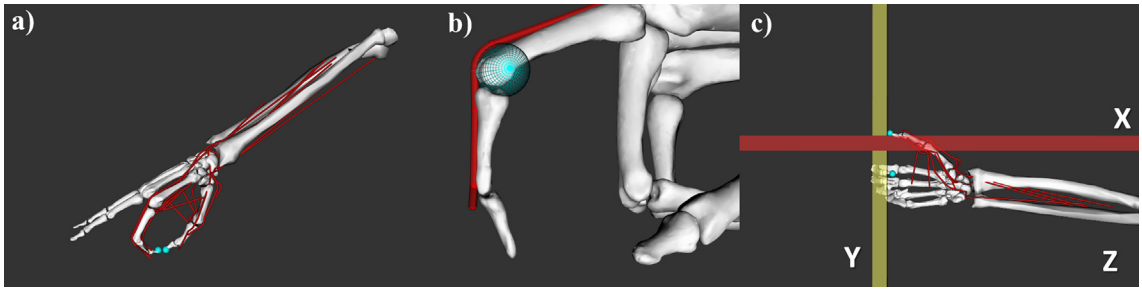

Fig. 1. OpenSim 3.3 model of hand generated for analyses. (A) All 7 index finger muscles and all 8 thumb muscles are represented in the model. (B) Frictionless, massless ellipsoids were used to produce the proper wrapping of tendons about joints and, thus, the correct moment arms. (C). Frictionless walls used to constrain the thumb tip and record force in all three orthogonal directions.

2.3. Estimation of effects of activation deficits on force production

The model was employed to examine the relative sensitivity of fingertip and thumb force production on activation deficits for each of the muscles. These muscle activation deficits are common following neurological injury such as stroke (Hoffmann et al., 2016, Li et al., 2014, Triandafilou et al., 2011). EMG patterns recorded from healthy adults served as the baseline patterns (Qiu and Kamper, 2014, Valero-Cuevas et al., 2003). Tip force was recorded for subsequent activation reductions from 100% to 0% (25% decrements) of baseline for each muscle.

3. Results

3.1. Model validation results

Fingertip and thumb-tip forces from model simulations were generally agreeable with reported experimental data (Qiu et al., 2017). Simulated force magnitudes for all index finger muscles in the sagittal plane were within ±1 SD of the corresponding experimental data (Fig. 2). Simulated force direction also fell within this range, except for flexor digitorum superficialis (FDS) and flexor digitorum profundus (FDP) which were slightly more distal than experimental data (0.9° and 4.4°, respectively). In the coronal plane, forces for only the intrinsic muscles were examined. Model force vectors matched experimental magnitudes for all three intrinsic muscles and direction for two of the three muscles. FDI force was 13.0° further in the ulnar direction than expected.

For the thumb, sagittal plane force directions largely matched the experimental data from the literature (Fig. 3). The model predictions in the coronal plane were not as accurate as the sagittal plane. The intrinsics had the largest errors in directional accuracy, with the predicted flexor pollicis brevis (FPB) vector rotated a further 26.1° toward adduction and the adductor pollicis longus (APL) vector rotated 12.1° into adduction. The extensors, extensor pollicis longus (EPL) and extensor pollicis brevis (EPB) showed the largest deviations in force magnitude (19% less and 48% greater than experimental, respectively).

Qualitatively, the model effectively simulated dynamic finger and thumb movements from experimentally recorded EMG data (see supplementary video clips). The movements exhibit proper coordination among joint rotations and the fingertip/thumb-tip motions are smooth and properly directed.

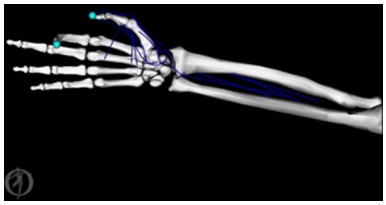

Video 1.

3.2. Simulating activation deficits

For the index finger, analysis performed using the model showed that force generation in the dorsal direction was most affected by variations in FDI activation. At 0% FDI activation, the dorsal force direction shifted by 83° compared to the baseline direction. Palmar force generation was most sensitive to FDP deficits, which changed the force direction by 60° and decreased the overall force magnitude from 7.7 N (100% activation) to 1.9 N (0% activation) (Supplementary Fig. 1.).

Supplementary data associated with this article can be found, in the online version, at https://doi.org/10.1016/j.jbiomech.2018.06.017.

Examination of the thumb muscles found that, in the dorsal direction, EPL most affected the direction (73.1° change) as well

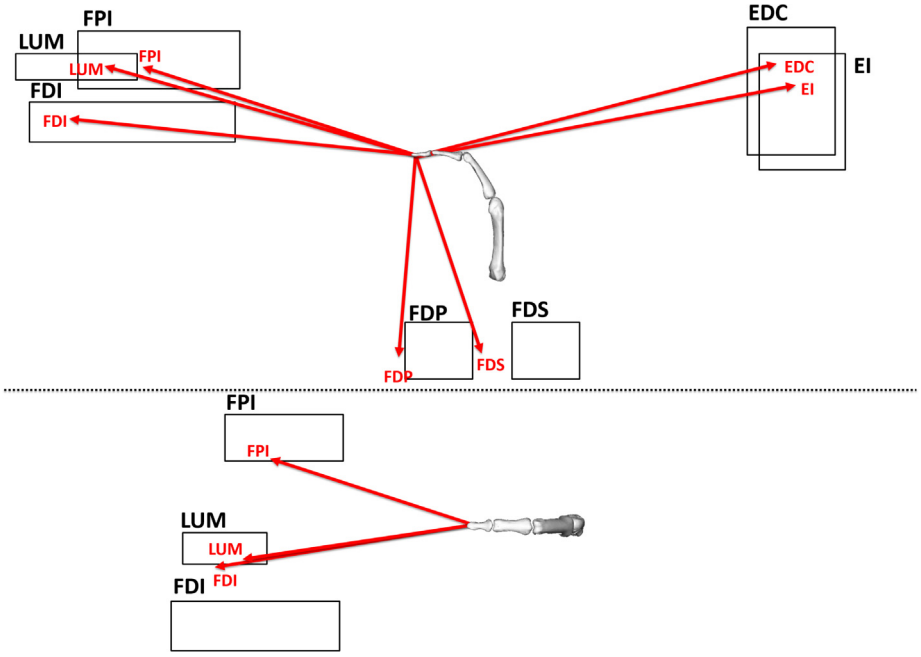

Fig. 2. Isometric force results for each of the index finger muscles in the sagittal (top) and coronal (bottom) planes. In the coronal plane, only force directions from the intrinsic index finger muscles were reported. Arrows indicate simulated force values; boxes indicate corresponding experimental values (mean ± 1 standard deviation in each orthogonal direction) (Qiu et al., 2017). Muscles included are: first dorsal interosseous (FDI), lumbrical (LUM), first palmar interosseous (FPI), extensor digitorum communis (EDC), extensor indicis (EI), flexor digitorum profundus (FDP), and flexor digitorum superficialis (FDS).

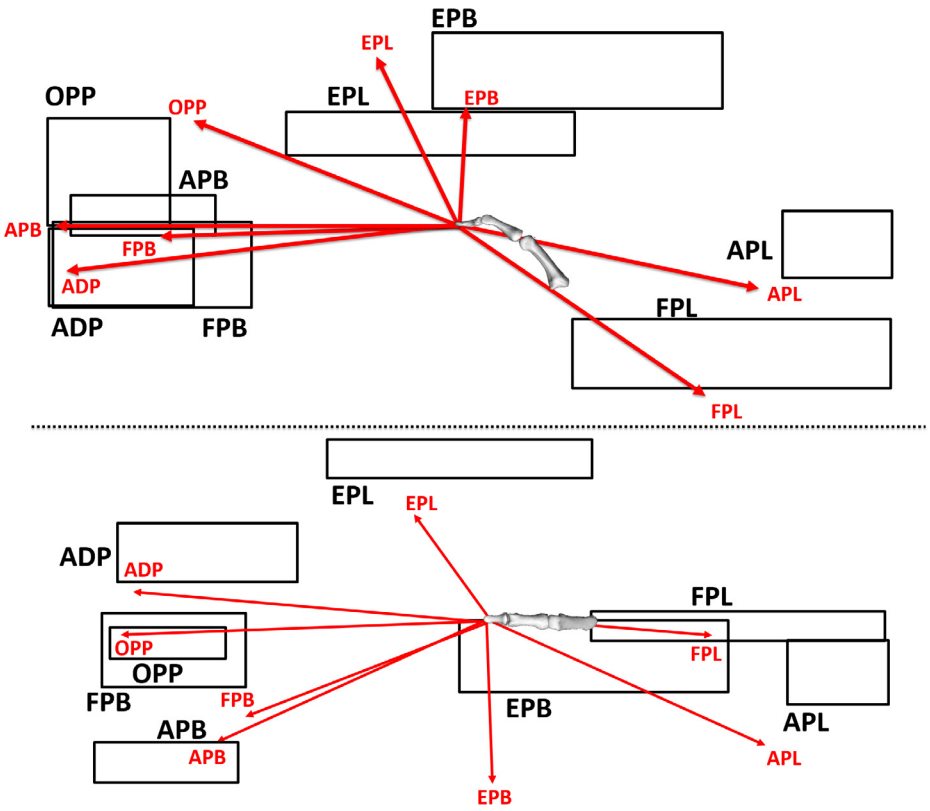

Fig. 3. Isometric force results for each of the thumb muscles in the sagittal (top) and coronal (bottom) planes. Arrows indicate simulated force values; boxes indicate corresponding force ranges from literature (50th percentile interquartile range in each orthogonal direction) (Towles et al., 2008). Muscles included are: adductor pollicis (ADP), flexor pollicis brevis (FPB), adductor pollicis brevis (APB), opponens pollicis (OPP), extensor pollicis longus (EPL), extensor pollicis brevis (EPB), adductor pollicis longus (APL), and flexor pollicis longus (FPL).

as force magnitude (from 12.7 N at 100% activation to 4.4 N at 0% activation). In the palmar direction, flexor pollicis longus (FPL) had the most profound impact on palmar force production, a decrease of 40.5 N at 50% activation; at this point, the force was almost entirely in the distal direction (see Supplementary material). ADP had the second largest effect on overall force production, causing a force decrease of 32 N at 0% activation (Supplementary Figs. 2 and 3).

4. Discussion

Comparison of isometric force generation of the dynamic hand model with cadaveric data from literature showed good correspondence. For the index finger, simulated fingertip force and magnitude resulting from loading individual tendons generally fell within the standard range of experimental data. In the sagittal plane, only force directions for FDS and FDP fell outside this range, and by less than 5°. In the coronal plane, discrepancy for FDI was greater, with the simulated force directed too far towards the ulna. Errors may have arisen from the difficulty in appropriately distributing force across the two heads of FDI to match forces applied during experiments.

Simulated and experimental force data for the thumb also generally matched, but not as closely as the index finger. The greatest discrepancies were observed for FPB direction in the coronal plane and magnitudes of EPB and EPL. Errors may have arisen from disparity in musculotendon parameters. Model parameter values, culled from multiple sources, may not have matched those of the cadaver specimens. Additionally, the complicated kinematics of the thumb make estimation of moment arms for each DOF quite challenging. Determination of "effective static moment arms" from relationships across multiple joints may further improve model accuracy (Lee et al., 2008, Qiu et al., 2017).

The dynamic simulations showed expected behavior with simultaneous rotation of joints within the same digit, although further quantitative validation with complete data sets is needed. The inclusion of passive stiffness and damping was necessary to appropriate movement within the model, as observed previously (Kamper et al., 2002, Lee et al., 2008). Unfortunately, literature values are not readily available for passive impedance of thumb MCP and IP joints.

Use of the model yielded insights about the sensitivity of force production from the index finger and thumb with activation pattern changes. While each muscle may be active during a force task (Qiu et al., 2009, Valero-Cuevas et al., 2003), the relative impact of each varies considerably. In the index finger, modelled deficits in FDI activation had an especially profound effect on force direction for production of both palmar and dorsal forces. This is strengthened by studies which have shown that FDI activation is impaired following stroke (Li et al., 2014). In the thumb, ADP showed the largest palmar force effects of all the muscles. These results suggest that FDI, ADP, and other intrinsics may be important targets for post-stroke rehabilitation. A more detailed analysis is found in Supplementary materials.

Thus, the validated model can provide important insight for the mapping from muscle activation to finger and thumb movement and force generation. This model however, is limited by the data sets which define the physiological parameters used. As variability between cadaveric samples may lead to discrepancies between

results, there may be merit in comparing this model to complete parameter sets from single cadavers (Goislard De Monsabert et al., 2018, Mirakhorlo et al., 2016). Simulation of activation deficits were constrained to activation patterns while physiological changes not examined here, such as excessive muscle co-activation, may have profound effects on force production. Further refinement of the model through improved estimation of effective moment arms, muscle physiological cross-sectional area, and passive stiffness should also lead to even better simulation capabilities to study motor control and its rehabilitation.

5. Conflict of interest

The authors of this paper have no conflicts of interest to report.

6. Author statement

All authors were fully involved in the study and preparation of the manuscript. The material within this manuscript has not been and will not be submitted for publication elsewhere. There is no conflict of interest in the submission of this manuscript.

Acknowledgements

Funding provided by NIDRR H133A140065.

References

Ajiboye, A.B., Weir, R.F., 2009. Muscle synergies as a predictive framework for the EMG patterns of new hand postures. J. Neural Eng. 6, 036004.
Almecija, S., Moya-Sola, S., Alba, D.M., 2010. Early origin for human-like precision grasping: a comparative study of pollical distal phalanges in fossil hominins. PLoS One 5, e11727.
An, K.N., Ueba, Y., Chao, E.Y., Cooney, W.P., Linscheid, R.L., 1983. Tendon excursion and moment arm of index finger muscles. J. Biomech. 16, 419–425.
Blana, D., Chadwick, E.K., van den Bogert, A.J., Murray, W.M., 2017. Real-time simulation of hand motion for prosthesis control. Comput. Methods Biomech. Biomed. Eng. 20, 540–549.
Buffi, J.H., Crisco, J.J., Murray, W.M., 2013. A method for defining carpometacarpal joint kinematics from three-dimensional rotations of the metacarpal bones captured in vivo using computed tomography. J. Biomech. 46, 2104–2108.
Delp, S.L., Anderson, F.C., Arnold, A.S., Loan, P., Habib, A., John, C.T., Guendelman, E., Thelen, D.G., 2007. OpenSim: open-source software to create and analyze dynamic simulations of movement. IEEE Trans. Biomed. Eng. 54, 1940–1950.
Domalain, M., Vigouroux, L., Berton, E., 2010. Determination of passive moment-angle relationships at the trapeziometacarpal joint. J. Biomech. Eng. 132, 071009.
Esteki, A., Mansour, J.M., 1997. A dynamic model of the hand with application in functional neuromuscular stimulation. Ann. Biomed. Eng. 25, 440–451.
Ficke, R.C., Science Management Corporation. and National Institute on Disability and Rehabilitation Research (U.S.), 1992. Digest of data on persons with disabilities. National Institute on Disability and Rehabilitation Research, Washington, D.C., pp.
Goislard De Monsabert, B., Edwards, D., Shah, D., Kedgley, A., 2018. Importance of consistent datasets in musculoskeletal modelling: a study of the hand and wrist. Ann. Biomed. Eng. 46, 71–85.
Hager-Ross, C., Schieber, M.H., 2000. Quantifying the independence of human finger movements: comparisons of digits, hands, and movement frequencies. J. Neurosci. 20, 8542–8550.
Hoffmann, G., Conrad, M.O., Qiu, D., Kamper, D.G., 2016. Contributions of voluntary activation deficits to hand weakness after stroke. Top Stroke Rehabil. 23, 384–392.
Hollister, A., Buford, W.L., Myers, L.M., Giurintano, D.J., Novick, A., 1992. The axes of rotation of the thumb carpometacarpal joint. J. Orthop. Res. 10, 454–460.
Hollister, A., Giurintano, D., 1993. How Joints Move. Mosby, St. Louis, MO., pp. 35–59.
Hollister, A., Giurintano, D.J., Buford, W.L., Myers, L.M., Novick, A., 1995. The axes of rotation of the thumb interphalangeal and metacarpophalangeal joints. Clin. Orthop Relat. Res., 188–193
Holzbaur, K.R., Murray, W.M., Delp, S.L., 2005. A model of the upper extremity for simulating musculoskeletal surgery and analyzing neuromuscular control. Ann. Biomed. Eng. 33, 829–840.
Jacobson, M.D., Raab, R., Fazeli, B.M., Abrams, R.A., Botte, M.J., Lieber, R.L., 1992. Architectural design of the human intrinsic hand muscles. J. Hand Surg. Am. 17, 804–809.
Kamper, D.G., George Hornby, T., Rymer, W.Z., 2002. Extrinsic flexor muscles generate concurrent flexion of all three finger joints. J. Biomech. 35, 1581–1589.
Klein Breteler, M.D., Simura, K.J., Flanders, M., 2007. Timing of muscle activation in a hand movement sequence. Cereb. Cortex 17, 803–815.
Knutson, J.S., Kilgore, K.L., Mansour, J.M., Crago, P.E., 2000. Intrinsic and extrinsic contributions to the passive moment at the metacarpophalangeal joint. J. Biomech. 33, 1675–1681.
Landsmeer, J.M., 1961. Studies in the anatomy of articulation. II. Patterns of movement of bi-muscular, bi-articular systems. Acta Morphol. Neerl. Scand. 3, 304–321.
Lee, S.W., Chen, H., Towles, J.D., Kamper, D.G., 2008. Estimation of the effective static moment arms of the tendons in the index finger extensor mechanism. J. Biomech. 41, 1567–1573.
Lee, S.W., Zhang, X., 2007. Biodynamic modeling, system identification, and variability of multi-finger movements. J. Biomech. 40, 3215–3222.
Li, X., Shin, H., Zhou, P., Niu, X., Liu, J., Rymer, W.Z., 2014. Power spectral analysis of surface electromyography (EMG) at matched contraction levels of the first dorsal interosseous muscle in stroke survivors. Clin. Neurophysiol. 125, 988–994.
Lieber, R.L., Jacobson, M.D., Fazeli, B.M., Abrams, R.A., Botte, M.J., 1992. Architecture of selected muscles of the arm and forearm: anatomy and implications for tendon transfer. J. Hand Surg. Am. 17, 787–798.
Millard, M., Uchida, T., Seth, A., Delp, S.L., 2013. Flexing computational muscle: modeling and simulation of musculotendon dynamics. J. Biomech. Eng. 135, 021005.
Mirakhorlo, M., Visser, J.M.A., Goislard de Monsabert, B.A.A.X., Helm, C.T.V.d., Maas, H., Veeger, H.E.J., 2016. Anatomical parameters for musculoskeletal modeling of the hand and wrist. Int. Biomech. 3, 40–49.
Mogk, J.P., Johanson, M.E., Hentz, V.R., Saul, K.R., Murray, W.M., 2011. A simulation analysis of the combined effects of muscle strength and surgical tensioning on lateral pinch force following brachioradialis to flexor pollicis longus transfer. J. Biomech. 44, 669–675.
Qiu, D., Fischer, H.C., Kamper, D.G., 2009. Muscle activation patterns during force generation of the index finger. Conf. Proc. IEEE Eng. Med. Biol. Soc. 2009, 3987–3990.
Qiu, D., Kamper, D.G., 2014. Orthopaedic Applications of a Validated Force-based Biomechanical Model of the Index Finger. IEEE Engineering in Medicine and Biology Society, Chicago, IL.
Qiu, D., Lee, S.W., Amine, M., Kamper, D.G., 2017. Intersegmental kinetics significantly impact mapping from finger musculotendon forces to fingertip forces. J. Biomech. 65, 82–88.
Sancho-Bru, J.L., Perez-Gonzalez, A., Vergara-Monedero, M., Giurintano, D., 2001. A 3-D dynamic model of human finger for studying free movements. J. Biomech. 34, 1491–1500.
Sancho-Bru, J.L., Perez-Gonzalez, A., Vergara, M., Giurintano, D.J., 2003. A 3D biomechanical model of the hand for power grip. J. Biomech. Eng. 125, 78–83.
Smutz, W.P., Kongsayreepong, A., Hughes, R.E., Niebur, G., Cooney, W.P., An, K.N., 1998. Mechanical advantage of the thumb muscles. J. Biomech. 31, 565–570.
Stamenkovic, A., Munro, B.J., Peoples, G.E., 2014. Physiological cross-sectional area of the oblique head of the adductor pollicis is greater than its transverse counterpart: implications for functional testing. Muscle Nerve 49, 405–412.
Thelen, D.G., Anderson, F.C., Delp, S.L., 2003. Generating dynamic simulations of movement using computed muscle control. J. Biomech. 36, 321–328.
Towles, J.D., Hentz, V.R., Murray, W.M., 2008. Use of intrinsic thumb muscles may help to improve lateral pinch function restored by tendon transfer. Clin. Biomech. (Bristol, Avon) 23, 387–394.
Triandafilou, K.M., Fischer, H.C., Towles, J.D., Kamper, D.G., Rymer, W.Z., 2011. Diminished capacity to modulate motor activation patterns according to task contributes to thumb deficits following stroke. J. Neurophysiol. 106, 1644–1651.
Triandafilou, K.M., Kamper, D.G., 2012. Investigation of hand muscle atrophy in stroke survivors. Clin. Biomech. (Bristol, Avon) 27, 268–272.
Valero-Cuevas, F.J., Johanson, M.E., Towles, J.D., 2003. Towards a realistic biomechanical model of the thumb: the choice of kinematic description may be more critical than the solution method or the variability/uncertainty of musculoskeletal parameters. J. Biomech. 36, 1019–1030.
Valero-Cuevas, F.J., Zajac, F.E., Burgar, C.G., 1998. Large index-fingertip forces are produced by subject-independent patterns of muscle excitation. J. Biomech. 31, 693–703.
Vignais, N., Cocchiarella, D.M., Kociolek, A.M., Keir, P.J., 2013. Dynamic Assessment of Finger Joint Loads Using Kinetic and Kinematic Measurements. Digital Human Modeling. Ann Arbor, Michigan.
Wohlman, S.J., 2015. Understanding the Dynamics of Thumb-tip Force Generation through Integration of Simulation and Experimanetal Methods. Northwestern University, Evanston, Illinois (Doctor of Philosophy).
Wohlman, S.J., Murray, W.M., 2013. Bridging the gap between cadaveric and in vivo experiments: a biomechanical model evaluating thumb-tip endpoint forces. J. Biomech. 46, 1014–1020.
Young, R.W., 2003. Evolution of the human hand: the role of throwing and clubbing. J. Anat. 202, 165–174.